frontiers in Materials

ORIGINAL RESEARCH
published: 02 March 2018
doi: 10.3389/fmats.2018.00011

Fabrication of Antibacterial Poly(Vinyl Alcohol) Nanocomposite Films Containing Dendritic Polymer Functionalized Multi-Walled Carbon Nanotubes

Andreas Sapalidis, Zili Sideratou*, Katerina N. Panagiotaki, Elias Sakellis, Evangelos P. Kouvelos, Sergios Papageorgiou and Fotios Katsaros*

Institute of Nanoscience and Nanotechnology, National Centre of Scientific Research Demokritos, Athens, Greece

OPEN ACCESS

Edited by:
Vasilios Georgakilas, University of Patras, Greece

Reviewed by:
Susanna Bosi, University of Trieste, Italy
Aristides Bakandritsos, Palacky University Olomouc, Czechia
Horacio Javier Salavagione, Consejo Superior de Investigaciones Científicas (CSIC), Spain

****Correspondence:***
Andreas Sapalidis
a.sapalidis@inn.demokritos.gr;
Zili Sideratou
z.sideratou@inn.demokritos.gr

Specialty section:
This article was submitted to Carbon-Based Materials, a section of the journal Frontiers in Materials

Received: *03 December 2017*
Accepted: *13 February 2018*
Published: *02 March 2018*

Citation:
Sapalidis A, Sideratou Z, Panagiotaki KN, Sakellis E, Kouvelos EP, Papageorgiou S and Katsaros F (2018) Fabrication of Antibacterial Poly(Vinyl Alcohol) Nanocomposite Films Containing Dendritic Polymer Functionalized Multi-Walled Carbon Nanotubes. Front. Mater. 5:11. doi: 10.3389/fmats.2018.00011

A series of poly(vinyl alcohol) (PVA) nanocomposite films containing quaternized hyperbranched polyethyleneimine (PEI) functionalized multi-walled carbon nanotubes (ox-CNTs@QPEI) are prepared by solvent casting technique. The modified carbon-based material exhibits high aqueous solubility, due to the hydrophilic character of the functionalized hyperbranched dendritic polymer. The quaternized PEI successfully wraps around nanotube walls as polycations provide electrostatic repulsion. Various contents of ox-CNTs@QPEI ranging from 0.05 to 1.0% w/w were employed to prepare functionalized PVA nanocomposites. The developed films exhibit adequate optical transparency, improved mechanical properties and extremely high antibacterial behavior due to the excellent dispersion of the functionalized CNTs into the PVA matrix.

Keywords: poly(vinyl alcohol), carbon-based nanofillers, nanocomposites, carbon nanotube, quaternized hyperbranched polyethyleneimine, antibacterial properties

INTRODUCTION

The use of carbon nanotubes (CNTs) as fillers in polymer nanocomposites development is in the focus of research, since their discovery in the early 1990s aiming at the enhancement of the mechanical and electrical properties on a vast array of polymeric matrices (Breuer and Sundararaj, 2004). The reason behind this extensive interest is the unique properties that CNTs exhibit, mainly their high tensile strength, originating from the perfect axial alignment of carbon–carbon covalent bonds, which ranges approximately from 11 to 63 GPa, for multi-walled CNTs (MWCNTs) (Yu et al., 2000). This value, an order on magnitude higher than that of carbon fibers, is accompanied also by higher aspect ratios (typically in the range of 100–10,000) and lower density (7 g cm^{-3} for the CNTs with regards to 9 g cm^{-3} for the carbon fibers). On the other hand for the single wall carbon nanotubes (SWCNTs), the tensile strength is in the range of 50–500 GPa, once again significantly higher than that of carbon fibers (Al-Saleh and Sundararaj, 2011). Apart from the improvement in mechanical strength, the unique electrical and thermal properties of CNTs make them ideal nanofillers for the development of conductive nanocomposites.

For such applications, dispersibility is a crucial parameter that determines their potential utilization: CNTs should be able to effectively disperse in a uniform fashion throughout the matrix, while maintaining their integrity and aspect ratio. Moreover, in order for load transfer across the CNT-matrix interface to be achieved, good interfacial bonding is necessary. However, CNTs tend to

aggregate severely, due to their high surface energy, minimizing their dispersability in solvents. To this end, several modification techniques have been proposed to achieve high CNTs dispersion in polymeric matrices. The most widely used approach is their surface modification by macromolecules. Polymeric chains, having good affinity with the carbon's surface groups, can wrap around the nanotube, altering completely the chemical compatibility of the hybrid increasing their dispersion in various solvents. The modification involves covalent (grafting) or non-covalent bonding (physical interactions) using either hydrophilic or hydrophobic polymers (Spitalsky et al., 2010). In the first case, the attachment of the macromolecules involves one or more chemical steps, while the second approach is carried out simply by mixing the CNTs with the appropriate polymer.

Poly(vinyl alcohol) (PVA) is a water-soluble synthetic polymer used in many applications extending from biomedical, such as orthopedic (Kobayashi and Hyu, 2010; Baker et al., 2012) and tissue engineering (Kumar and Han, 2017) to everyday uses, such as in the paper industry (Xu et al., 2006; Awada et al., 2015), electronics (Bettinger and Bao, 2010; Van Etten et al., 2014), textiles (Halima, 2016), and printing (Angjellari et al., 2017). All these sectors benefit from PVA's unique properties, including excellent film formation, resistance to organic solvents, gas barrier properties, especially to oxygen, adhesive properties, biocompatibility, and to some extent, biodegradability (Chiellini et al., 2003). PVA-based composites have been developed in the past using various fillers like inorganic oxides (Yang, 2007; Dodda et al., 2015), clays (Strawhecker and Manias, 2000; Podsiadlo et al., 2007; Sapalidis et al., 2012), CNTs (Shaffer and Windle, 1999; Paiva et al., 2004; Ciambelli et al., 2005; Liu et al., 2005; Bhattacharya et al., 2006; Miaudet et al., 2007; Minus et al., 2010; Surdo et al., 2011; Li et al., 2013), graphene oxide (Salavagione et al., 2009a; Zhao et al., 2010; Swati et al., 2015; Ma et al., 2016), reduced graphene oxide (Salavagione et al., 2009b; Pourjavadi et al., 2015; Manna et al., 2016), or biomaterials (Sapalidis et al., 2007), all targeting to significantly improve the mechanical and thermal stability along with gas permeability, while trying to preserve the excellent optical transparency of PVA. As mentioned previously, the key parameter for successful preparation of polymer nanocomposites is the effective filler dispersion.

Regarding the preparation of PVA/CNTs composites several studies have been reported. Shaffer and Windle fabricated a series of PVA/CNTs nanocomposites (10–60%), and measured the thermomechanical and electrical properties of the developed films (Shaffer and Windle, 1999). Paiva et al. (2004) prepared functionalized CNTs/PVA composites, with nanotubes well dispersed into the PVA matrix affording films with higher strength compared to parent PVA films. Liu et al. (2005) prepared PVA films with functionalized SWCNTs with excellent optical transparency due to enhanced CNTs–polymer interactions. Ciambelli et al. (2005) examined the properties of PVA/CNTs and noticed a shift in the glass transition temperature (T_g) followed by a delay in the thermal oxidation of PVA. Bhattacharya et al. (2006) used denatured collagen in order to increase the dispersion of SWCNTs in a PVA matrix. The developed composites exhibited increased crystallinity and enhanced mechanical properties. Miaudet et al. (2007) developed PVA/CNTs fibers for conductive and multifunctional textile applications. Minus et al. (2010) studied the crystallization of PVA in the presence of SWCNTs and they suggested that PVA molecules are aligned parallel to the SWNT axis. Surdo et al. (2011) studied the gas barrier properties of PVA/SWCNTs films for both hydrophobic organic and heavy metal pollutants.

More recently, PVA/CNTs nanocomposites were introduced in a variety of applications, such as bio-inspired composite yarns (Beese et al., 2013), dye sensitized solar cells (Nath et al., 2014), polymer electrolyte fuel cells (Sayeed et al., 2014), electroactive shape memory polymers (Du et al., 2015), and humidity sensors (Manohara et al., 2016). However, despite the well reported antibacterial activity of CNTs and the vast variety of their applicability (Kang et al., 2008; Liu et al., 2009; Dizaj et al., 2015), there has been a limited number of literature reports regarding the potential use of PVA/CNTs composites, as antibacterial films.

In this study, oxidized multi-walled nanotubes were functionalized with quaternized hyperbranched polyethyleneimine (QPEI) through non-covalent interactions affording a hydrophilic hybrid material—ox-CNTs@QPEI—compatible with hydrophilic PVA. Subsequently, a series of PVA nanocomposite films containing ox-CNTs@QPEI up to 1% were prepared by solvent casting technique. The average sample thickness was 120 ± 15 μm. The nanocomposite films were thoroughly investigated employing X-ray diffraction, electron microscopy, thermogravimetric analysis, mechanical properties, differential scanning calorimetry (DSC), and UV–vis spectroscopy. All applied techniques revealed the excellent dispersion of the functionalized CNTs into PVA matrix. Additionally, the antibacterial activities of the as-prepared films were assessed against Gram-negative bacteria displaying exceptional antibacterial properties.

MATERIALS AND METHODS

Materials

Hyperbranched polyethyleneimine (PEI) having a molecular weight of 25,000 Da (Lupasol® WF, water-free, 99%), was kindly provided by BASF (Ludwigshafen, Germany). Low viscosity, partially hydrolyzed atactic PVA Mowiol 8–88 with an average molecular weight 67,000 g mol^{-1} was purchased by Fluka Analytical. Glycidyltrimethylammonium chloride, triethylamine, and dialysis tubes (molecular weight cut-off: 1,200) were purchased from Sigma-Aldrich Ltd. (Poole, UK). Oxidized multi-walled CNTs containing carboxyl groups >8% w/w (ox-CNTs) with mean diameter × mean length: 9.5 nm × 1.5 μm were purchased from Sigma-Aldrich. Ultra-pure water was used for all preparations. A 10% w/w PVA stock solution in water was prepared by stirring the appropriate polymer amount for 6 h at 90°C and used for the preparation of all composites.

Synthesis of QPEI

A quaternized derivative of hyperbranched PEI with 50% degree of substitution was prepared by an analogous method previously described (Sideratou et al., 2000). Briefly, an aqueous solution (10 mL) containing 24 mmol glycidyltrimethylammonium chloride and 48 mmol triethylamine, was added to 0.2 mmol PEI with molecular weight 25,000 Da dissolved in 40 mL water. The mixture was stirred for several hours, and purified by dialysis

against deionized water, using a 1,200 cut-off membrane. The final product, QPEI, was received after lyophilization and its structure was confirmed by NMR spectroscopy. The degree of quaternization was calculated by ^{1}H-NMR spectrum and it was found to be 50%.

Preparation of QPEI-Functionalized ox-CNTs

In a typical experiment, 50 mg of ox-CNTs were dispersed in 50 mL QPEI aqueous solution (3 mg mL^{-1}). The mixture was ultasonicated for 15 min using a standard sonotrode (3 mm tip-diameter), in a Hielscher UP200S high intensity ultrasonic processor, at 50% amplitude, and 0.5 cycles and left to stir for further 12 h, at room temperature. The final product was received after ultracentrifugation at 45,000 rpm, followed by lyophilization affording the hybrid ox-CNTs@QPEI material.

Preparation of PVA/ox-CNTs@QPEI Nanocomposites

The samples were prepared by simple mixing of a stock ox-CNTs@QPEI dispersion (10 mg mL^{-1}) with PVA stock solution (10% w/w) at various ratios, in order to obtain dry PVA films with 0.05, 0.10, 0.25, 0.5, and 1.0% w/w functionalized nanotubes loading. The mixtures were ultrasonicated for 30 min and then stirred for 24 h at room temperature. The as-prepared suspensions (15–25 mL with regards to the final film thickness) were transferred to square polystyrene Petri dishes (120 × 120 mm), and the dry films were obtained after slow water evaporation at 22–25°C, for 15 days. The resulting dry nanocomposite films had an average thickness of 120 ± 15 μm and were used without any further treatment for all characterization methods.

Physicochemical Characterization of ox-CNTs@QPEI and PVA/ox-CNTs@QPEI Nanocomposite Films

Raman spectra were recorded with a micro-Raman system RM 1000 Renishaw, employing a laser excitation line at 532 nm (Nd-YAG), in the range of 400–2,000 cm^{-1}. Thermogravimetric analysis (TGA) was performed on a Setaram SETSYS Evolution 17 instrument, at a 5°C min^{-1} heating rate under oxygen atmosphere. The thermal properties of the films were measured employing a modulated DSC model 2920 TA instrument. Heating scans were carried out from 25 to 250°C at a rate of 5°C min^{-1}. Prior the first heating cycle, a pretreatment up to 120°C was carried out, to remove the weakly adsorbed water. In order to avoid any thermal memory of the samples and to minimize the effect of strongly adsorbed water, after the first heating, a cooling cycle was performed, followed by a second heating cycle up to 250°C. Heating at higher temperatures led to the decomposition of the PVA nanocomposites in agreement with previous studies (Yang, 2007; Mohsin et al., 2011). The thermodynamic parameters T_g, T_m, and ΔH_m were calculated from both heating cycles. Scanning Electron Microscopy (SEM) images were obtained by a Jeol JSM 7401 F Field Emission Scanning Electron Microscope with Gentle Beam mode. Gentle Beam reduces charging, resulting in improved resolution, signal-to-noise, and beam brightness, especially at low beam voltages (down to 0.1 kV). Transmission electron micrographs were obtained using a Philips C20 TEM instrument operating at an accelerating voltage of 200 kV. For the preparation of TEM samples, a drop of 1% PVA/ox-CNTs@QPEI aqueous solution was casted on a PELCO® Formvar grid and was left to evaporate. ζ-potential measurements of the aqueous ox-CNTs@QPEI dispersion (0.05 mg mL^{-1}) were conducted using a ZetaPlus −Brookhaven Instruments Corp. UV–vis spectra of the aqueous ox-CNTs@QPEI dispersion (1 mg mL^{-1}) were recorded by a Cary 100 Conc UV–visible spectrophotometer (Varian Inc.) operating in the range of 200–800 nm. Additionally, the colloid stability of the aqueous dispersion was evaluated at static condition for 1, 6, and 12 months. Specifically, the dispersions obtained as mentioned previously and stored at room temperature. At each time point, an aliquot of 200 μL was taken from the upper part of the dispersions, diluted to 1 mL water, and their optical density (OD) was measured using UV–vis spectroscopy.

Tensile tests were performed using a Thumler GmbH Tensile Tester Model equipped with a PA 6110 Nordic Transducer load cell at room temperature with a maximum force of 250 N. For all samples, a crosshead speed of 50 mm min^{-1} was used. The specimens' length was 12 cm, the effective length (i.e., distance between the grips) was 8 cm, while their width was 1 cm. Before the measurements, the samples were pre-equilibrated for 48 h at ambient temperature and humidity. A Siemens XD-500 diffractometer with a CuK_{a1} radiation source was employed to record X-ray diffraction patterns of the samples, with a scan rate of 0.03 s^{-1}, using background-free holders.

Antibacterial Assessment Assay

The *in vitro* antibacterial activity of PVA/ox-CNTs@QPEI nanocomposites was screened against the Gram-negative *Escherichi Coli* bacteria. *E. coli* was cultured in lambda broth (LB) medium containing tryptone 10 g L^{-1}, yeast extract 5 g L^{-1}, and NaCl 10 g L^{-1} (pH = 7.5) at 37°C for 16 h, on a rotary shaker at approximately 200 rpm shaking speed. The *E. coli* bacteria were harvested at the mid-exponential growth and centrifuged at 1,500 *g* for 5 min. Then, the pellet was washed twice and re-suspended in LB medium. Bacterial suspensions were obtained after dilution to an OD of 0.4 recorded at 500 nm, corresponding to final cells concentration of 10^4 colony forming units per mL (CFU mL^{-1}). *E. coli* inoculums were incubated for 30 min in the presence of various PVA/ox-CNTs@QPEI dispersions containing 10% PVA and 0.05, 0.1, 0.25, 0.5, or 1% w/w ox-CNTs@QPEI with respect to PVA. The bacterial growth was monitored by measuring the OD values at 500 nm every 2 h on a Cary 100 Conc UV–visible spectrophotometer (Varian Inc.). For comparison, the antibacterial activity of pure PVA was studied under the same conditions with the nanocomposites. All experiments were performed in triplicates.

RESULTS AND DISCUSSION

Water soluble dendritic polymer functionalized CNTs, ox-CNTs@QPEI, was developed by physical (non-covalent) interactions between the oxidized CNTs and the QPEI, in aqueous media. This hybrid nanomaterial was characterized by Raman, TGA, and SEM. Specifically, the typical graphite bands at 1,585 cm^{-1}

(G band), 1,345 cm^{-1} (D band), and ~2,700 cm^{-1} ("G" band) ascribed to the in-plane vibration of the sp^2-bonded carbon atoms in the graphite layers, to the presence of defects in carbon systems, and to the overtone of the D band, respectively, are shown in the RAMAN spectra of ox-CNTs and QPEI-functionalized ox-CNTs (**Figure 1**). Comparing the RAMAN shifts of functionalized ox-CNTs with those of ox-CNTs, no significant changes can be noticed, which signifies that only limited changes on the ox-CNTs structure occurred during functionalization. The only change that can be observed relates to the intensity ratio value of G- to D-bands (I_G/I_D) that increases from 1.04 to 1.13, indicating successful polymer wrapping around CNTs (Wepasnick et al., 2010).

The TGA graphs are presented in **Figure 2**. In the case of ox-CNTs, the low temperature (below 300°C) weight loss is a result

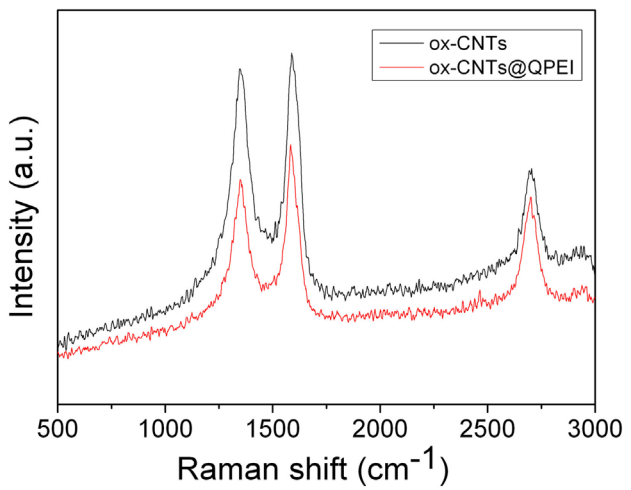

FIGURE 1 | Raman spectra of ox-carbon nanotubes (ox-CNTs) (black) and ox-CNTs@QPEI (red).

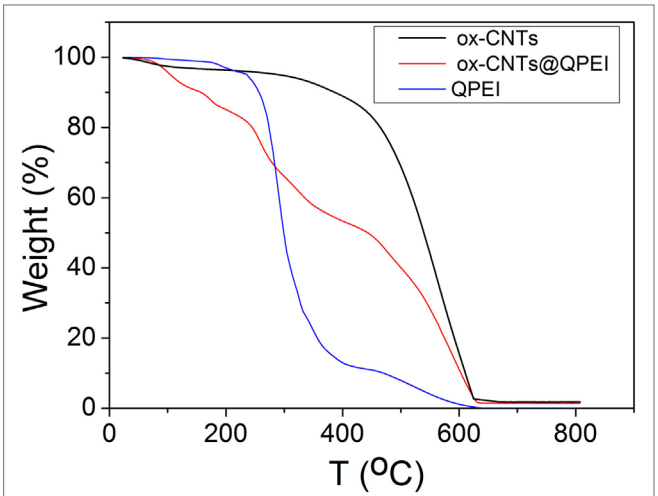

FIGURE 2 | Thermogravimetric profiles of oxidised-carbon nanotubes (ox-CNTs) (black), quaternized hyperbranched polyethyleneimine (QPEI) (blue), and ox-CNTs@QPEI (red) measured in air.

of the decomposition of the oxygen containing groups, while at high temperatures (>500°C), thermal destruction of the graphitic framework is observed. The QPEI shows a significant mass loss in the range between 200 and 400°C, followed by a second decomposition region around 450°C. Regarding the ox-CNTs@QPEI curve, two main distinct decomposition regions are observed. The first one (below 400°C) can be attributed to the QPEI degradation together with the removal of CNTs' oxygen groups, while the second (above 400°C) is related to the damage of the graphitic framework. At higher temperatures (above 600°C), all organic components are fully decomposed, while the residual mass can be attributed to the metal catalyst used for CNTs production, as well as the oxidation products of these catalysts (Lehman et al., 2011). Based on the analysis in this region, the polymer loading on CNTs was found to be 21.4%.

Further direct evidence for the functionalization of ox-CNTs can be obtained by SEM. As revealed by SEM images, the surface of ox-CNTs is quite smooth (**Figure 3**, left image), while after functionalization with QPEI, the surface of the hybrid appears to be rougher, exhibiting a debundled structure (**Figure 3**, middle and right). It is obvious that the functionalized CNTs are less prone to aggregation and they seem to be well-dispersed and isolated.

Furthermore, the evaluation of CNTs' aqueous colloidal stability was achieved by UV–vis spectroscopy. It is known that only individual CNTs are absorbed in the UV–vis region, while the bundled CNTs are not active in this region (Yu et al., 2007). **Figure 4** shows the UV–vis spectra of the aqueous dispersions of ox-CNTs and ox-CNTs@QPEI, recorded in the region of 200–800 nm. The higher absorption of the characteristic peak at 263 nm attributed to the *p*-plasmon absorption of carbon nanomaterials, confirms the efficient de-bundling of ox-CNTs by QPEI. Additionally, the de-bundling of ox-CNTs was also corroborated by the presence of scattering in the UV spectra (Yu et al., 2007). Stable dispersions of ox-CNTs@QPEI were obtained for at least 12 months (**Figure 5**), due to the presence of positively charged quaternary ammonium groups, at the external surface of CNTs. These groups increase the CNTs compatibility to aqueous media due to their strong hydrophilicity and also prevent CNTs' aggregation owing to electrostatic repulsion.

Surface net charge for ox-CNTs and ox-CNTs@QPEI aqueous dispersions was determined at pH = 7.0. The obtained ζ-potential values are −34 mV and +52 mV, respectively. The change of the ζ-potential values suggests that the positive charged QPEI was successfully attached onto the graphitic framework. It is known that colloidal systems with a ζ-potential value greater than +30 mV are quite stable due to efficient electrostatic repulsions (Schierz and Zänker, 2009; Bhattacharjee, 2016). In the case of ox-CNTs@QPEI, this value is much higher than +30 mV signifying stable aqueous CNTs dispersion, in agreement with the results of UV–vis measurements (see above).

Poly(vinyl alcohol) nanocomposites films were prepared with various ox-CNTs@QPEI content ranging from 0.05 to 1% w/w by employing the common solvent-casting technique. Films of ca. 120 ± 15 μm thickness were obtained and used for further characterization.

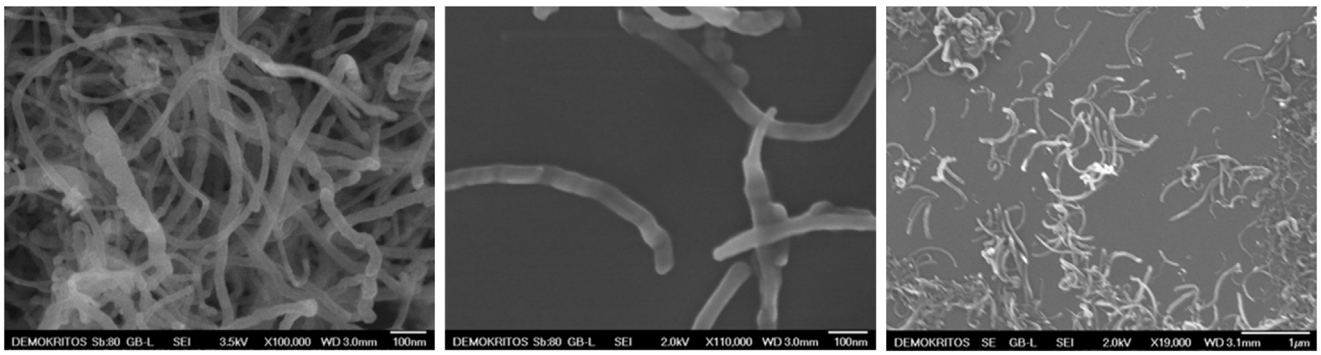

FIGURE 3 | Scanning electron microscopy images of oxidised-carbon nanotubes (ox-CNTs) (left) and ox-CNTs@QPEI (middle and right).

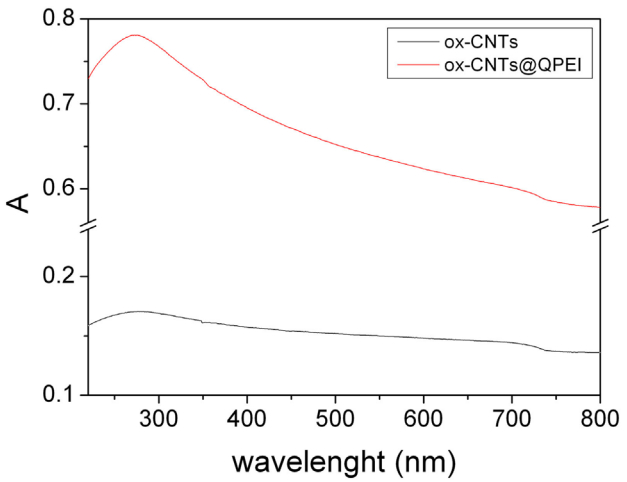

FIGURE 4 | UV–vis absorption spectra of oxidised-carbon nanotubes (ox-CNTs) (black) and ox-CNTs@QPEI (red), in aqueous solution (1 mg mL^{-1}).

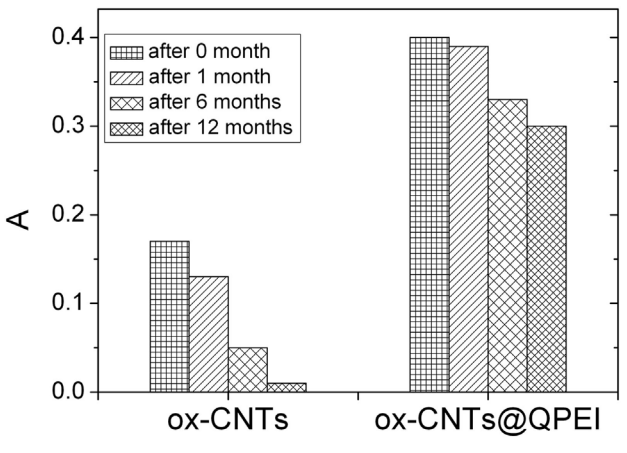

FIGURE 5 | Sedimentation behavior of oxidised-carbon nanotubes (ox-CNTs) and ox-CNTs@QPEI at different aging time.

Transmission electron microscopy is one of the most extensively used method to identify the polymer nanocomposite structure and the dispersion of the nanofillers. **Figure 6** shows TEM micrographs of the PVA/ox-CNTs@QPEI 1% nanocomposite film. It can be noticed that the functionalized nanotubes are well dispersed in the PVA matrix, since individual ox-CNTs@QPEI can be clearly observed with dimensions ranging from 1 to 8 μm in length and ~30 nm in width.

The optical clarity of the nanocomposites can be used to indirectly evaluate the dispersion of CNTs into transparent polymer matrices, like PVA, as the high optical clarity of the nanocomposites, indicates the excellent dispersion in nanoscale. As shown in the transmittance spectra, **Figure 7**, at higher wavenumbers, the nanocomposite films with CNTs loading up to 0.1% retain almost 75% of the optical transparency of the pure PVA, revealing an effective dispersion of nanotubes into the PVA matrix. Increase in the CNTs loading (up to 0.25%) causes further reduction in optical clarity. Finally, at higher CNTs loading (up to 1%) a significant decrease in transmittance is observed. It should be noted that even at 120 μm film thicknesses, the optical transparency is highly retained (47% transmission reduction in the case of 0.5% loading) in contrast to a previous study, where PVA composites films containing 0.5% SWCNTs exhibited transmission reduction around 78% with a film thickness of only 50 μm (Li et al., 2013). These results are in line with the results derived from TEM analysis. The absorbance observed at 284 and 327 nm can be assigned to $\pi \rightarrow \pi^*$ transitions of the unsaturated bonds C = O and C = C bonds located at the tail head of the PVA (El-Kader, 2003). As the ox-CNTs@QPEI concentration increases, these features almost disappeared, since CNTs are known to exhibit strong absorption in this region (Zhang et al., 2016).

The decreased UV transmittance for all samples, in the region below 420 nm, demonstrates that the addition of functionalized CNTs improves the UV blocking properties of the nanocomposites. This can be attributed to both the increased absorbance of CNTs in the region, due to $\pi \rightarrow \pi^*$ transition, and the good dispersion of the nanofillers into PVA (Hu et al., 2017).

Differential scanning calorimetry along with wide angle X-ray diffraction can reveal crucial information about the structure and quality of crystals in semicrystalline polymers. It is known that

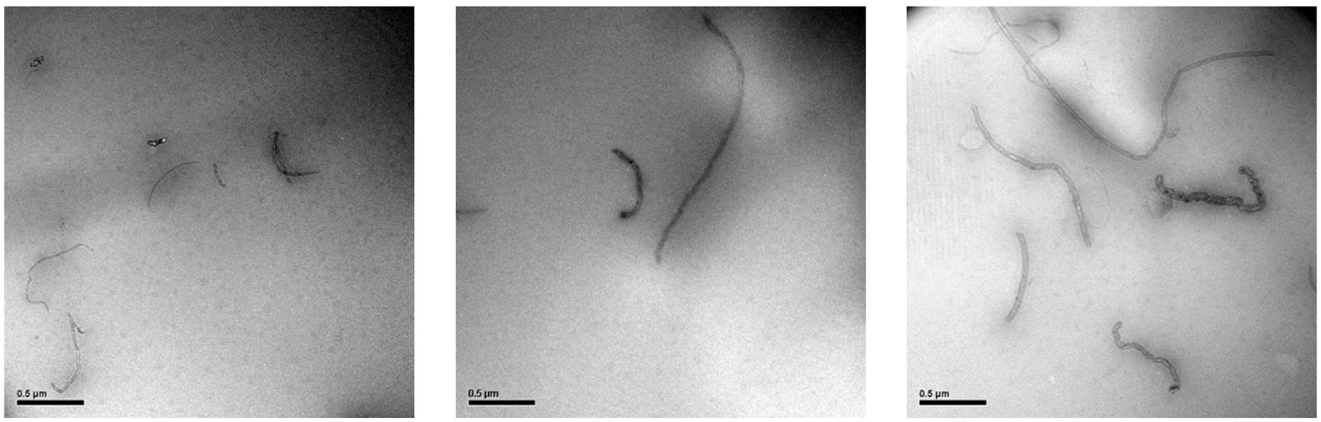

FIGURE 6 | TEM micrographs of PVA/ox-CNTs@QPEI 1.0% nanocomposite film.

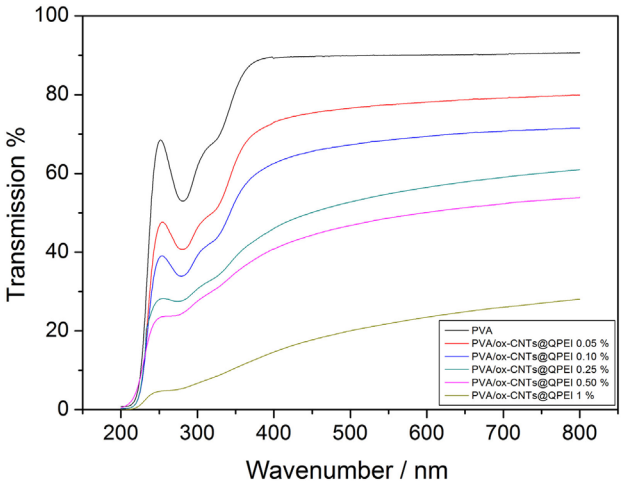

FIGURE 7 | UV–vis spectra of pure poly(vinyl alcohol) (PVA) film and PVA/ox-CNTs@QPEI nanocomposite films.

the crystal formation in PVA is a result of the intermolecular hydrogen bonding between the hydroxyl groups of PVA chains (Hodge et al., 1996). Therefore, hydrogen bonds between polymer and fillers can affect PVA crystallinity, as fillers can act as nucleation points for crystal formation. The thermal properties of PVA/ox-CNTs@QPEI nanocomposite films were studied by DSC to investigate the effect of functionalized carbon filler on melting temperature (T_m), melting enthalpy (ΔH), and degree of crystallinity (% X_c) of PVA. DSC diagrams of pure PVA and PVA/ox-CNTs@QPEI nanocomposites are shown in **Figure 8** and the results are summarized in **Table 1**.

During the first heating cycle only minor changes were observed in T_m values, while the crystallinity of PVA in nanocomposites is slightly reduced. In the second heating, the nanocomposite films exhibited higher melting temperatures (T_m), together with increased melting ΔH. In the latter case, the removal of water molecules that participate to PVA crystals causes a decrease in the crystallinity of pure PVA sample. In the case of nanocomposites, a slight increase in both melting temperatures and enthalpies is observed, indicating only a slight effect of functionalized CNTs on crystal structure of PVA. Similarly, the (T_g)s are more pronounced in second heating cycle (**Table 1**). The small decrease in T_g that it is observed for the nanocomposites implies rather weak polymer-functionalized CNTs interactions (Bhattacharya, 2016).

The synergy between the functionalized CNTs and the PVA, in nanoscale, is governed by the extent of the interfacial area and the strength of the interactions between the available functional groups. In the case of ox-CNTs@QPEI, the type of available external groups (primary amines and quaternary groups) together with the small surface area, limit the effect of CNTs on PVA crystallization. This result is in line with the conclusions derived for PVA nanocomposites with low graphene oxide content (Hu et al., 2017). On the contrary, the fillers can affect the PVA crystallization in the case of clay/PVA composites, due to enhanced interaction area and increased density of functional groups on inorganic platelets (Sapalidis et al., 2011).

Similarly, no significant alterations are observed in X-ray diffractograms of the pure PVA and PVA/ox-CNTs@QPEI nanocomposite films (**Figure 9**). Specifically, the X-ray patterns of PVA/ox-CNTs@QPEI nanocomposites are the same with that of pure PVA, since only the characteristic broad peaks of PVA at $2\theta = 19.4°$, 22.5°, and 40.8° attributed to the (1,0,1), (1,0,−1), and (2,2,0) crystal planes are shown (Singhal et al., 2012). Hence, the results from both techniques are in line indicating that the interaction between the functionalized CNTs and PVA is relatively weak, retaining the crystal structure of PVA almost unaffected.

The effect of functionalized nanotubes on the PVA thermal decomposition and stability was investigated *via* thermogravimetric analysis of PVA and all functionalized nanocomposite films. Three distinct decomposition steps are observed in the TGA profile of pure PVA (**Figure 10**), in the 40–110, 240–390, and 390–480°C ranges, attributed to the removal of physically absorbed water, the decomposition of hydroxyl groups of PVA, and the decomposition of the polymeric backbone, respectively (Hodge et al., 1996). Analogous decomposition steps are observed in the TGA profile of PVA/ox-CNTs@QPEI nanocomposite films (**Figure 10**). In general only small changes are observed.

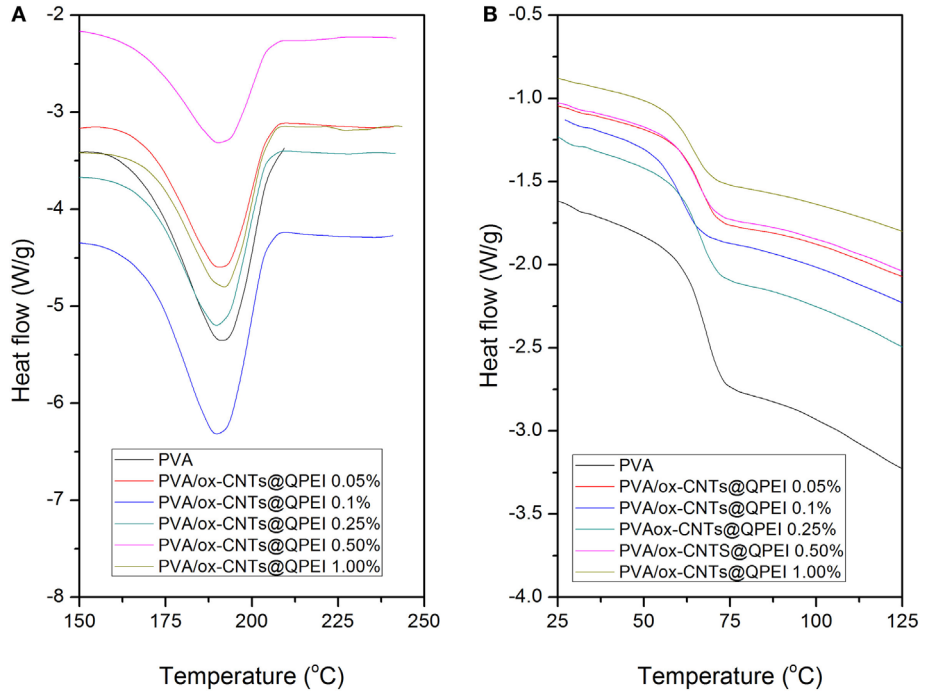

FIGURE 8 | Differential scanning calorimetry curves of the pure poly(vinyl alcohol) (PVA) and the PVA/ox-CNTs@QPEI nanocomposite films **(A)** first heating cycle (melting region) and **(B)** second heating cycle (glass transition region).

TABLE 1 | Melting temperature (T_m), glass transition temperature (T_g), enthalpy (ΔH), and degree of crystallinity (X_c)[a] of the developed nanocomposite films.

	1st heating			2nd heating			
Sample	T_m/°C	ΔH/J g^{-1}	%X_c[a]	T_g/°C	T_m/°C	ΔH/J g^{-1}	%X_c[a]
PVA	191.24	34.93	25.13	71.70	179.25	16.87	12.14
PVA/ox-CNTs@QPEI 0.05%	190.83	31.89	22.94	67.84	176.92	24.64	17.73
PVA/ox-CNTs@QPEI 0.10%	190.00	30.08	21.64	63.15	183.33	29.89	21.50
PVA/ox-CNTs@QPEI 0.25%	189.97	29.24	21.04	67.76	184.07	20.08	14.45
PVA/ox-CNTs@QPEI 0.50%	190.32	32.89	23.66	67.36	185.22	23.00	16.55
PVA/ox-CNTs@QPEI 1.0%	192.22	28.93	20.81	63.57	191.22	18.51	13.32

[a]X_c100% = 139.00 J g^{-1} (Peresin et al., 2010).

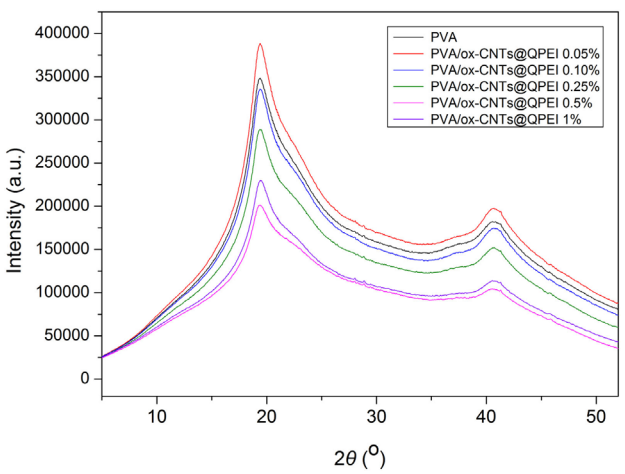

FIGURE 9 | X-ray diffractograms of the functionalized poly(vinyl alcohol) nanocomposite films.

Specifically, the weight loss slightly decreases with increasing content of the functionalized CNTs into the PVA matrix, while the thermal decomposition temperatures are shifted to marginally higher values.

Furthermore, the analysis of the tensile properties can reveal structural information in nanoscale. Poorly dispersed fillers will result in deterioration of both tensile strength and modulus of elasticity. In principle, the overall behavior is governed by the weakest structural point, which in the case of composites, is the interface between filler and polymer. The obtained results of materials' mechanical testing show a 50.67% improvement on the Young's modulus for the sample with 0.25% ox-CNTs@QPEI loading, in comparison to the pure PVA sample (**Table 2**). It must be noted that the mechanical properties enhancement upon addition of CNTs is due to the increased dispersion of the fillers in the matrix and cannot be attributed to the observed crystallinity changes. Further, increase in filler loading leads to decreased mechanical performance. Since, TEM analysis confirmed the absence of CNTs aggregates, the observed deterioration can be

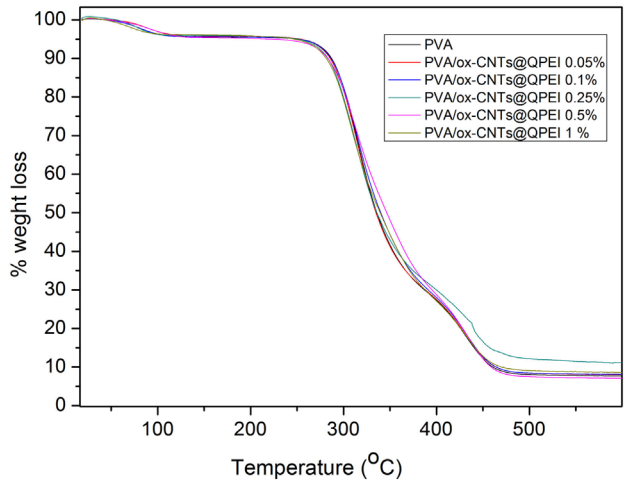

FIGURE 10 | Thermogravimetric profiles of poly(vinyl alcohol) (PVA) and PVA/ox-CNTs@QPEI nanocomposite films.

attributed to limited PVA/functionalized CNTs interactions. Additionally, the ultimate tensile strength values follow the same trend. Specifically, in the case of 0.25% ox-CNTs@QPEI loading, the tensile strength increases from 50.03 to 84.23 MPa a 68.35% increase compared to the pure PVA, while higher CNTs loading lead to decreased performance (**Table 2**).

The antibacterial activity of the PVA/ox-CNTs@QPEI nanocomposites was investigated against Gram-negative *E. coli* bacterial cells. Bacteria were cultured until logarithmic growth was achieved, and then PVA nanocomposites with various ox-CNTs@QPEI loading ranging from 0.05–1% w/w were added to the media. The turbidity of the prepared solutions was monitored for 12 h and the resulting cytotoxicities are shown in **Figure 11**. As expected, pure PVA was not toxic to *E. coli* bacteria, while enhanced antibacterial activity for the PVA/ox-CNTs@QPEI nanocomposites was observed through the amplitude of the sigmoidal curve, which was comparatively compressed. It must be noted that, in contrast to previous reports (Dadfar et al., 2014), where enhanced antibacterial properties were obtained using high CNTs loading (1–4%), in this study, the antibacterial performance can be attained using very low CNTs content (0.1%), while fully antibacterial protection can be achieved by adding only 0.25% ox-CNTs@QPEI in the PVA matrix.

Previous studies have shown that both SWCNTs and MWCNTs can be used as antibacterial agents, while the proposed mechanisms of their activity include reactive oxidative stress, blocking of intracellular metabolic routes, and rupture of cell membrane (Akhavan and Ghaderi, 2010). However, their agglomeration defines their overall antimicrobial activity, altering their shape and surface area (Wick et al., 2007).

On the other hand, it is known that both quaternary ammonium derivatives (Russel, 1969) and multi-walled CNTs (Kang et al., 2008; Liu et al., 2009; Dizaj et al., 2015) present significant antibacterial activity against both Gram-positive and Gram-negative bacteria. However, in the concentration range used in this study,

TABLE 2 | Mechanical properties of poly(vinyl alcohol) (PVA) and nanocomposite films.

Sample	Young modulus		Tensile strength	
	GPa	Difference	MPa	Difference
PVA	2.52 ± 0.31	–	50.03 ± 8.4	–
PVA/ox-CNTs@QPEI 0.1%	3.05 ± 0.79	21.03%	68.33 ± 19.5	36.58%
PVA/ox-CNTs@QPEI 0.25%	3.80 ± 0.85	50.67%	84.23 ± 19.7	68.35%
PVA/ox-CNTs@QPEI 0.50%	2.26 ± 0.69	−10.19%	42.09 ± 16.1	−15.87%
PVA/ox-CNTs@QPEI 1.0%	2.27 ± 0.55	−10.03%	41.23 ± 11.6	−17.60%

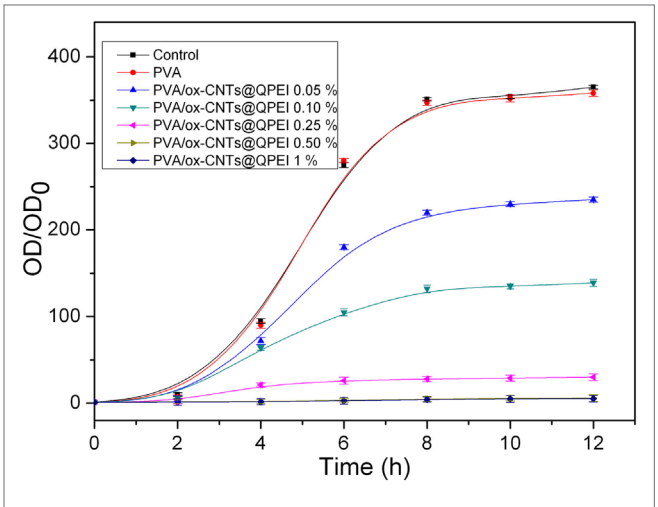

FIGURE 11 | Growth curves of Gram-negative *E. coli* bacteria incubated in the presence of PVA/ox-CNTs@QPEI nanocomposites. The control was bacteria treated with distilled water.

QPEI does not show any antibacterial activity (EC_{50} = 710 μg/mL). The role of QPEI is dual: (i) enhancing the CNTs solubility and (ii) forming positively charged hybrids (ox-CNTs@QPEI). It is known that CNTs functionalized with positively charged groups show increased ability to kill bacteria due to their strong interaction with the bacterial membranes that increases the permeability across the membrane (Zardini et al., 2012). Therefore, the presence of hybrid ox-CNTs@QPEI material, which combines both positively charged groups of quaternary ammonium and CNTs, induces the antibacterial properties of PVA composites, even at low filler content. This may occur due to the strong interaction of the hybrid material with the bacterial membranes, leading to membrane disruption and bacterial death.

CONCLUSION

Oxidized multi-walled CNTs decorated with QPEI (ox-CNTs@QPEI) were successfully prepared and physicochemically characterized. The aqueous colloid stability of ox-CNTs@QPEI was evaluated by UV–vis spectroscopy and was found that the hybrid's aqueous dispersions exhibit stability for extremely long

periods. A series of PVA films containing various ox-CNTs@QPEI concentrations were prepared by the solvent casting technique. Morphological analysis of nanocomposites by TEM revealed the excellent dispersion of the functionalized CNTs into PVA. In close agreement with TEM analysis, the adequate optical transparency of the films further supported this conclusion. At low loadings (up to 0.25%), the composite films exhibit enhanced mechanical strength, which, however, decreased at higher CNTs loading. Regarding the thermal properties, only marginal changes in comparison to the pure PVA were observed. Finally, the nanocomposite samples exhibited significant antibacterial properties, depending on the ox-CNTs@QPEI loading, making them candidate materials for a vast variety of applications, including textiles, biomedical, and food industry.

AUTHOR CONTRIBUTIONS

All authors contributed, wrote, and edited the paper.

FUNDING

Partial funding support by EU under the FP7 PEOPLE-2012-IAPP-SANAD project (No 324443) is acknowledged (http://www.sanadproject.eu/).

REFERENCES

Akhavan, O., and Ghaderi, E. (2010). Toxicity of graphene and graphene oxide nanowalls against bacteria. *ACS Nano* 4, 5731–5736. doi:10.1021/nn101390x

Al-Saleh, M. H., and Sundararaj, U. (2011). Review of the mechanical properties of carbon nanofiber/polymer composites. *Composites Part A* 42, 2126–2142. doi:10.1016/j.compositesa.2011.08.005

Angjellari, M., Tamburri, E., Montaina, L., Natali, M., Passeri, D., Rossi, M., et al. (2017). Beyond the concepts of nanocomposite and 3D printing: PVA and nanodiamonds for layer-by-layer additive manufacturing. *Mater. Des.* 119, 12–21. doi:10.1016/j.matdes.2017.01.051

Awada, H., Bouatmane, M., and Daneault, C. (2015). High strength paper production based on esterification of thermomechanical pulp fibers in the presence of poly(vinyl alcohol). *Heliyon* 1, e00038. doi:10.1016/j.heliyon.2015.e00038

Baker, M. I., Walsh, S. P., Schwartz, Z., and Boyan, B. D. (2012). A review of polyvinyl alcohol and its uses in cartilage and orthopedic applications. *J. Biomed. Mater. Res. B Appl. Biomater.* 100, 1451–1457. doi:10.1002/jbm.b.32694

Beese, A. M., Sarkar, S., Nair, A., Naraghi, M., An, Z., Moravsky, A., et al. (2013). Bio-inspired carbon nanotube-polymer composite yarns with hydrogen bond-mediated lateral interactions. *ACS Nano* 7, 3434–3446. doi:10.1021/nn400346r

Bettinger, C. J., and Bao, Z. (2010). Organic thin-film transistors fabricated on resorbable biomaterial substrates. *Adv. Mater.* 2, 651–655. doi:10.1002/adma.200902322

Bhattacharjee, S. (2016). DLS and zeta potential – what they are and what they are not? *J. Control Release* 235, 337–351. doi:10.1016/j.jconrel.2016.06.017

Bhattacharya, S. (2016). Polymer nanocomposites—a comparison between carbon nanotubes, graphene, and clay as nanofillers. *Materials* 9, 262. doi:10.3390/ma9040262

Bhattacharya, S., Salvetat, J.-P., and Saboungi, M.-L. (2006). Reinforcement of semicrystalline polymers with collagen-modified single walled carbon nanotubes. *Appl. Phys. Lett.* 88, 233119. doi:10.1063/1.2209187

Breuer, O., and Sundararaj, U. (2004). Big returns from small fibers: a review of polymer/carbon nanotube composites. *Polym. Compos.* 25, 630–645. doi:10.1002/pc.20058

Chiellini, E., Corti, A., D'Antone, S., and Solaro, R. (2003). Biodegradation of poly (vinyl alcohol) based materials. *Prog. Polym. Sci.* 28, 963–1014. doi:10.1016/S0079-6700(02)00149-1

Ciambelli, P., Sarno, M., Gorrasi, G., Sannino, D., Tortora, M., and Vittoria, V. (2005). Preparation and physical properties of carbon nanotubes-PVA nanocomposites. *J. Macromol. Sci., Phys.* 44, 779–795. doi:10.1080/00222340500251410

Dadfar, S. M. M., Kavoosi, G., and Dadfar, S. M. A. (2014). Investigation of mechanical properties, antibacterial features, and water vapor permeability of polyvinyl alcohol thin films reinforced by glutaraldehyde and multiwalled carbon nanotube. *Polym. Compos.* 35, 1736–1743. doi:10.1002/pc.22827

Dizaj, S. M., Mennati, A., Jafari, S., Khezri, K., and Adibkia, K. (2015). Antimicrobial activity of carbon-based nanoparticles. *Adv. Pharm. Bull.* 5, 19–23. doi:10.5681/apb.2015.003

Dodda, J. M., Belsky, P., Chmelar, J., Remis, T., Smolna, K., Tomas, M., et al. (2015). Comparative study of PVA/SiO2 and PVA/SiO2/glutaraldehyde (GA) nanocomposite membranes prepared by single-step solution casting method. *J. Mater. Sci.* 50, 6477–6490. doi:10.1007/s10853-015-9206-7

Du, F.-P., Ye, E.-Z., Yang, W., Shen, T.-H., Tang, C.-Y., Xie, X.-L., et al. (2015). Electroactive shape memory polymer based on optimized multi-walled carbon nanotubes/polyvinyl alcohol nanocomposites. *Composites Part B* 68, 170–175. doi:10.1016/j.compositesb.2014.08.043

El-Kader, K. M. A. (2003). Spectroscopic behavior of poly(vinyl alcohol) films with different molecular weights after UV irradiation, thermal annealing, and double treatment with UV irradiation and thermal annealing. *J. Appl. Polym. Sci.* 88, 589–594. doi:10.1002/app.11743

Halima, N. B. (2016). Poly(vinyl alcohol): review of its promising applications and insights into biodegradation. *RSC Adv.* 6, 39823–39832. doi:10.1039/C6RA05742J

Hodge, R. M., Bastow, T. J., Edward, G. H., Simon, G. P., and Hill, A. J. (1996). Free volume and the mechanism of plasticization in water-swollen poly(vinyl alcohol). *Macromolecules* 29, 8137–8143. doi:10.1021/ma951073j

Hu, X., Ren, N., Chao, Y., Lan, H., Yan, X., Sha, Y., et al. (2017). Highly aligned graphene oxide/poly(vinyl alcohol) nanocomposite fibers with high-strength, antiultraviolet and antibacterial properties. *Composites Part A* 102, 297–304. doi:10.1016/j.compositesa.2017.08.015

Kang, S., Herzberg, M., Rodrigues, D. F., and Elimelech, M. (2008). Antibacterial effects of carbon nanotubes: size does matter! *Langmuir* 24, 6409–6413. doi:10.1021/la800951v

Kobayashi, M., and Hyu, H. S. (2010). Development and evaluation of polyvinyl alcohol-hydrogels as an artificial atrticular cartilage for orthopedic implants. *Materials* 3, 2753–2771. doi:10.3390/ma3042753

Kumar, A., and Han, S. S. (2017). PVA-based hydrogels for tissue engineering: a review. *Int. J. Polym. Mater. Polym. Biomater.* 66, 159–182. doi:10.1080/00914037.2016.1190930

Lehman, J. H., Terrones, M., Mansfield, E., Hurst, K. E., and Meunier, V. (2011). Evaluating the characteristics of multiwall carbon nanotubes. *Carbon N. Y.* 49, 2581–2602. doi:10.1016/j.carbon.2011.03.028

Li, C., Lv, X., Dai, J., Cui, J., and Yan, Y. (2013). Synthesis of water-soluble single-walled carbon nanotubes and its application in poly(vinyl alcohol) composites. *Polym. Adv. Technol.* 24, 376–382. doi:10.1002/pat.3091

Liu, L., Barber, A. H., Nuriel, S., and Wagner, H. D. (2005). Mechanical properties of functionalized single-walled carbon-nanotube/poly(vinyl alcohol) nanocomposites. *Adv. Funct. Mater.* 15, 975–980. doi:10.1002/adfm.200400525

Liu, S. B., Wei, L., Hao, L., Fang, N., Chang, M. W., Xu, R., et al. (2009). Sharper and faster "nano darts" kill more bacteria: a study of antibacterial activity of individually dispersed pristine single-walled carbon nanotube. *ACS Nano* 3, 3891–3902. doi:10.1021/nn901252r

Ma, J., Li, Y., Yin, X., Xu, Y., Yue, J., Bao, J., et al. (2016). Poly(vinyl alcohol)/graphene oxide nanocomposites prepared by in situ polymerization with enhanced mechanical properties and water vapor barrier properties. *RSC Adv.* 6, 49448. doi:10.1039/C6RA08760D

Manna, K., Srivastava, S. K., and Mittal, V. (2016). Role of enhanced hydrogen bonding of selectively reduced graphite oxide in fabrication of poly(vinyl alcohol) nanocomposites in water as EMI shielding material. *J. Phys. Chem. C* 120, 17011–17023. doi:10.1021/acs.jpcc.6b03356

Manohara, S. R., Samal, S. S., and Rudreshappa, G. E. (2016). Humidity sensing properties of multiwalled carbon nanotubepolyvinyl alcohol nanocomposite films. *Nanosci. Nanotechn. – Asia* 6, 128–134. doi:10.2174/2210681206666160328201458

Miaudet, P., Bartholome, C., Derré, A., Maugey, M., Sigaud, G., Zakri, C., et al. (2007). Thermo-electrical properties of PVA-nanotube composite fibers. *Polymer* 48, 4068–4074. doi:10.1016/j.polymer.2007.05.028

Minus, M. L., Chae, H. G., and Kumar, S. (2010). Observations on solution crystallization of polyvinyl alcohol in the presence of single-wall carbon nanotubes. *Macromol. Rapid Commun.* 31, 310–316. doi:10.1002/marc.200900539

Mohsin, M., Hossin, A., and Haik, Y. (2011). Thermal and mechanical properties of poly(vinyl alcohol) plasticized with glycerol. *J. Appl. Polym. Sci.* 122, 3102–3109. doi:10.1002/app.34229

Nath, B. C., Gogoi, B., Boruah, M., Sharma, S., Khannam, M., Ahmed, G. A., et al. (2014). High performance polyvinyl alcohol/multi walled carbon nanotube/polyaniline hydrogel (PVA/MWCNT/PAni) based dye sensitized solar cells. *Electrochim. Acta* 146, 106–111. doi:10.1016/j.electacta.2014.08.134

Paiva, M. C., Zhou, B., Fernando, K. A. S., Lin, Y., Kennedy, J. M., and Sun, Y.-P. (2004). Mechanical and morphological characterization of polymer-carbon nanocomposites from functionalized carbon nanotubes. *Carbon N. Y.* 42, 2849–2854. doi:10.1016/j.carbon.2004.06.031

Peresin, M. S., Habibi, Y., Zoppe, J. O., Pawlak, J. J., and Rojas, O. J. (2010). Nanofiber composites of polyvinyl alcohol and cellulose nanocrystals: manufacture and characterization. *Biomacromolecules* 11, 674–681. doi:10.1021/bm901254n

Podsiadlo, P., Kaushik, A. K., Arruda, E. M., Waas, A. M., Shim, B. S., Xu, J., et al. (2007). Ultrastrong and stiff layered polymer nanocomposites. *Science* 318, 80–83. doi:10.1126/science.1143176

Pourjavadi, A., Pourbadiei, B., Doroudian, M., and Azari, S. (2015). Preparation of PVA nanocomposites using salep-reduced graphene oxide with enhanced mechanical and biological properties. *RSC Adv.* 5, 92428. doi:10.1039/C5RA12190F

Russel, A. D. (1969). The mechanism of action of some antibacterial agents. *Prog. Med. Chem.* 6, 135–199. doi:10.1016/S0079-6468(08)70198-X

Salavagione, H. J., Gómez, M. A., and Martínez, G. (2009a). Polymeric modification of graphene through esterification of graphite oxide and poly(vinyl alcohol). *Macromolecules* 42, 6331–6334. doi:10.1021/ma900845w

Salavagione, H. J., Martínez, G., and Gómez, M. A. (2009b). Synthesis of poly(vinyl alcohol)/reduced graphite oxide nanocomposites with improved thermal and electrical properties. *J. Mater. Chem.* 19, 5027–5032. doi:10.1039/b904232f

Sapalidis, A. A., Katsaros, F. K., and Kanellopoulos, N. K. (2011). "PVA/montmorillonite nanocomposites: development and properties," in *Nanocomposites and Polymers with Analytical Methods*, ed. Cuppoletti John (InTech), 29–50.

Sapalidis, A. A., Katsaros, F. K., Romanos, G. E., Kakizis, N. K., and Kanellopoulos, N. K. (2007). Preparation and characterization of novel poly-(vinyl alcohol)-Zostera flakes composites for packaging applications. *Composites Part B* 38, 398–404. doi:10.1016/j.compositesb.2006.04.005

Sapalidis, A. A., Katsaros, F. K., Steriotis, T. A., and Kanellopoulos, N. K. (2012). Properties of poly(vinyl alcohol)-bentonite clay nanocomposite films in relation to polymer-clay interactions. *J. Appl. Polym. Sci.* 123, 1812–1821. doi:10.1002/app.34651

Sayeed, M. D. A., Talukdar, K., Kim, H. J., Park, Y., Gopalan, A. I., Kim, Y. H., et al. (2014). Passive approach for the improved dispersion of polyvinyl alcohol-based functionalized multi-walled carbon nanotubes/Nafion® membranes for polymer electrolyte membrane fuel cells. *J. Nanosci. Nanotechnol.* 14, 9329–9334. doi:10.1166/jnn.2014.10125

Schierz, A., and Zänker, H. (2009). Aqueous suspensions of carbon nanotubes: surface oxidation, colloidal stability and uranium sorption. *Environ. Pollut.* 157, 1088–1094. doi:10.1016/j.envpol.2008.09.045

Shaffer, M. S. P., and Windle, A. H. (1999). Fabrication and characterization of carbon nanotube/poly(vinyl alcohol) composites. *Adv. Mater.* 11, 937–941. doi:10.1002/(SICI)1521-4095(199908)11:11<937::AID-ADMA937>3.0.CO;2-9

Sideratou, Z., Tsiourvas, D., and Paleos, C. M. (2000). Quaternized poly(propylene imine) dendrimers as novel p*H*-sensitive controlled release systems. *Langmuir* 16, 1766–1769. doi:10.1021/la990829v

Singhal, A., Kaur, M., Dubey, K. A., Bhardwaj, Y. K., Jain, D., Pillai, C. G. S., et al. (2012). Polyvinyl alcohol–In2O3 nanocomposite films: synthesis, characterization and gas sensing properties. *RSC Adv.* 2, 7180–7189. doi:10.1039/c2ra20416a

Spitalsky, Z., Tasis, D., Papagelis, K., and Galiotis, C. (2010). Carbon nanotube-polymer composites: chemistry, processing, mechanical and electrical properties. *Prog. Polym. Sci.* 35, 357–401. doi:10.1016/j.progpolymsci.2009.09.003

Strawhecker, K. E., and Manias, E. (2000). Structure and properties of poly(vinyl alcohol)/Na+ montmorillonite nanocomposites. *Chem. Mater.* 12, 2943–2949. doi:10.1021/cm000506g

Surdo, E. M., Khan, I. A., Choudhury, A. A., Saleh, N. B., and Arnold, W. A. (2011). Barrier properties of poly(vinyl alcohol) membranes containing carbon nanotubes or activated carbon. *J. Hazard. Mater.* 188, 334–340. doi:10.1016/j.jhazmat.2011.01.130

Swati, G., Vaibhav, K., Garima, A., and Prafulla, K. J. (2015). Synthesis and characterization of PVA/GO nanocomposite films. *Macromol. Symp.* 357, 173–177. doi:10.1002/masy.201400220

Van Etten, E. A., Ximenes, E. S., Tarasconi, L. T., Garcia, I. T. S., Forte, M. M. C., and Boudinov, H. (2014). Insulating characteristics of polyvinyl alcohol for integrated electronics. *Thin Solid Films* 568, 111–116. doi:10.1016/j.tsf.2014.07.051

Wepasnick, K. A., Smith, B. A., Bitter, J. L., and Fairbrother, D. H. (2010). Chemical and structural characterization of carbon nanotube surfaces. *Anal. Bioanal. Chem.* 396, 1003–1014. doi:10.1007/s00216-009-3332-5

Wick, P., Manser, P., Limbach, L. K., Dettlaff-Weglikowska, U., Krumeich, F., Roth, S., et al. (2007). The degree and kind of agglomeration affect carbon nanotube cytotoxicity. *Toxicol. Lett.* 168, 121–131. doi:10.1016/j.toxlet.2006.08.019

Xu, G. G., Yang, C. Q., and Deng, Y. (2006). Mechanism of paper wet strength development by polycarboxylic acids with different molecular weight and glutaraldehyde/poly(vinyl alcohol). *J. Appl. Polym. Sci.* 101, 277–284. doi:10.1002/app.23298

Yang, C.-C. (2007). Synthesis and characterization of the cross-linked PVA/TiO2 composite polymer membrane for alkaline DMFC. *J. Mem. Sci.* 288, 51–60. doi:10.1016/j.memsci.2006.10.048

Yu, J., Grossiord, N., Koning, C. E., and Loos, J. (2007). Controlling the dispersion of multi-wall carbon nanotubes in aqueous surfactant solution. *Carbon N. Y.* 45, 618–623. doi:10.1016/j.carbon.2006.10.010

Yu, M.-F., Lourie, O., Dyer, M. J., Moloni, K., Kelly, T. F., and Ruoff, R. S. (2000). Strength and breaking mechanism of multiwalled carbon nanotubes under tensile load. *Science* 287, 637–640. doi:10.1126/science.287.5453.637

Zardini, H. Z., Amiri, A., Shanbedi, M., Maghrebi, M., and Baniadam, M. (2012). Enhanced antibacterial activity of amino acids-functionalized multi walled carbon nanotubes by a simple method. *Colloids Surf. B Biointerfaces* 92, 196–202. doi:10.1016/j.colsurfb.2011.11.045

Zhang, W., Chen, M., Gong, X., and Diao, G. (2016). Universal water-soluble cyclodextrin polymer-carbon nanomaterials with supramolecular recognition. *Carbon N. Y.* 61, 154–163. doi:10.1016/j.carbon.2013.04.079

Zhao, X., Zhang, Q., and Chen, D. (2010). Enhanced mechanical properties of graphene-based poly(vinyl alcohol) composites. *Macromolecules* 43, 2357–2363. doi:10.1021/ma902862u

Conflict of Interest Statement: The authors declare that the research was conducted in the absence of any commercial or financial relationships that could be construed as a potential conflict of interest.